Simultaneous Acquisition of Microscale Reflectance and Normals

Supplemental Material #1

Giljoo Nam[†] Joo Ho Lee[†] Hongzhi Wu[§] Diego Gutierrez[*] Min H. Kim[†]

[†]KAIST [§]Zhejiang University, State Key Lab of CAD & CG [*]Universidad de Zaragoza, I3A

1 Reconstructing Reflectance and Normals

We describe our algorithm for jointly reconstructing both non-parametric SVBRDFs and normals, from our microscopic measurements, based on the Torrance-Sparrow model [1967]. Since we apply the traditional two-level concept of object and microfacet geometry to our microscopic measurements, we introduce a new layer of random irregularities in specular reflection at submicron resolution. We model this distribution as a *non-parametric* tabular function. Finally, we factorize the captured appearance into basis BRDFs and blending coefficients, which allows for accurate reproduction and editing of material appearance.

1.1 Reflectance Representation

We express the BRDF at each point $\mathbf{x}$ adapting the non-parametric version of the Torrance-Sparrow model, since this model does not depend on the particular distribution being used:

$$R(\mathbf{x},\mathbf{o},\mathbf{i}) = \frac{1}{\pi}\rho_d(\mathbf{x}) + \rho_s(\mathbf{x})\frac{D(\mathbf{x},\mathbf{h})G(\mathbf{n},\mathbf{o},\mathbf{i})F(\mathbf{x},\mathbf{h},\mathbf{i})}{4(\mathbf{n}\cdot\mathbf{o})(\mathbf{n}\cdot\mathbf{i})}, \qquad (1)$$

where ρ_d and ρ_s are diffuse and specular albedos at microfacet scale, $\mathbf{n}$ is the normal at $\mathbf{x}$ (the normal map has μm resolution), $\mathbf{h} = (\mathbf{o}+\mathbf{i})/|\mathbf{o}+\mathbf{i}|$ is the half-angle vector. D is the facet distribution term, G is the geometric term, and F is the Fresnel term, all of which will be detailed later in this section.

Specular Irregularity Our NDF is represented as a non-parametric tabulation function of 90 coefficients. We factorize the specular lobe as a single non-parametric NDF D with the monotonicity constraint only, following Ren et al. [2011]. The non-parametric coefficients are found from approx. two million lighting samples. These large number of lighting samples make our problem an overdetermined system, thus they are sufficient to determine non-parametric coefficients even *without smoothness constraints*. We found that smoothness constraints attenuate the specular highlight in the lobe.

Traditional BRDF models formulate the microfacet distribution as a parametric function [Cook and Torrance 1982; Ashikhmin et al. 2000]. However, the parametric function in that resolution is unknown. Instead, we leverage the capabilities of our capture system and follow a data-driven approach, formulating this unknown distribution D as a tabulated 1D array of 90 coefficients. Our distribution satisfies $D(\mathbf{x},\mathbf{h}) \geqslant 0$ and $\int_{\Omega_+}(\mathbf{h}\cdot\mathbf{n})D(\mathbf{x},\mathbf{h})dw_h = 1$, where $\Omega_+ = \Omega_+(\mathbf{n}) = \{\mathbf{h}|\mathbf{h}\cdot\mathbf{n} > 0\}$. We then extend this 1D array to non-parametric bases of spatially-varying BRDF through linearly constrained factorization [Lawrence et al. 2006].

Nanofacet Shadowing/Masking We formulate the shadowing/masking effects on both the light and view directions as $G(\mathbf{n},\mathbf{o},\mathbf{i}) = g(\mathbf{n},\mathbf{o})g(\mathbf{n},\mathbf{i})$. To account for the distribution in geometrical shadowing, we rely on Ashikhmin's formulation [2000] to our measured resolution:

$$g(\mathbf{n},\mathbf{k}) = \frac{(\mathbf{n}\cdot\mathbf{k})}{\int_{\Omega'_+}(\mathbf{h}\cdot\mathbf{k})D(\mathbf{h})d\omega_h}, \qquad (2)$$

where $\mathbf{k}$ is either $\mathbf{o}$ or $\mathbf{i}$. Note that g includes the integral of the nanofacet distribution D over the hemisphere $\Omega'_+ = \{\Omega_+(\mathbf{k}) \cap \Omega_+(\mathbf{n})\}$. Since this formulation relates the shadowing/masking G and the distribution D functions, we apply an alternating optimization approach for the factorization of both terms. Instead of merely initiating G with a constant [Ngan et al. 2005], we first calculate the initial G based on V-grooves [Cook and Torrance 1982]: $G(\mathbf{n},\mathbf{o},\mathbf{i}) = \min\left\{1, \frac{2(\mathbf{n}\cdot\mathbf{h})(\mathbf{n}\cdot\mathbf{o})}{(\mathbf{o}\cdot\mathbf{h})}, \frac{2(\mathbf{n}\cdot\mathbf{h})(\mathbf{n}\cdot\mathbf{i})}{(\mathbf{i}\cdot\mathbf{h})}\right\}$, and then factorize the basis BRDFs; this results in the initial D. In the following iterations, we update G by using Equation (2) and the estimated D. We found that this approach improves the convergence speed significantly (see Subsection 1.3 for optimization details).

Fresnel To determine the Fresnel term, we require a prior knowledge about the material properties, such as the refractive index or $F(0)$. Many recent works set the $F(0)$ term manually [Holroyd et al. 2008; Aittala et al. 2013; Ngan et al. 2005]. Given our form-factor constraints, we do not in general capture grazing angles beyond 45 degrees, where $F(0)$ remains virtually constant [Wang et al. 2011]. To reduce complexity during the optimization, we simplify $F(\mathbf{x},\mathbf{h},\mathbf{i})$ as a constant color vector F per BRDF basis.

1.2 Light Transport Formulation

We now describe how to relate the unknown microscale SVBRDF to our captured HDR images. The reflected radiance L at a point $\mathbf{x}$ along the view direction $\mathbf{o}$ under one directional light from $\mathbf{i}$ can be computed as

$$L(\mathbf{x},\mathbf{o}) = R(\mathbf{x},\mathbf{o},\mathbf{i})(\mathbf{n}\cdot\mathbf{i})L(\mathbf{x},\mathbf{i}). \qquad (3)$$

Let $\mathbf{l} \in \mathbb{R}^J$ be a vector representing the captured *per-pixel* radiance under J different light sources, and $\mathbf{r} \in \mathbb{R}^J$ be a vector of the corresponding per-pixel reflectances. From Equation (3), we have

$$\mathbf{l} = \boldsymbol{\phi} \odot \mathbf{r}, \qquad (4)$$

where $\boldsymbol{\phi} \in \mathbb{R}^J$ is the incident light times the cosine term $(\mathbf{n}\cdot\mathbf{i})$, and $\odot$ is the Hadamard product operator.

Observe that in Equation (1), R can be uniquely determined once ρ_d and the product $\rho_s FD$ are known, since none of the other terms depend on the material properties. To represent R, we can then use a *reflectance coefficient* vector $\boldsymbol{\gamma} = [\rho_d, \rho_s FD]^\intercal \in \mathbb{R}^M$ (where the length of $\rho_s FD$ is $M-1$). Now computing R essentially becomes solving for $\boldsymbol{\gamma}$.

Once we obtain $\boldsymbol{\gamma}$, we can factorize $\rho_s FD$ into the normalized distribution function D and the specular albedo times the Fresnel constants $\rho_s F$, by normalizing $\rho_s FD$ with $k_D = \int_\Omega \rho_s FD(\mathbf{h})(\mathbf{h}\cdot\mathbf{n})d\omega_h$ [Ashikhmin et al. 2000]. This normalized distribution D will be used for rendering later.

From Equation (1), defining a matrix $\boldsymbol{\Psi} = [\boldsymbol{\psi}_1, \cdots, \boldsymbol{\psi}_J]^\intercal \in \mathbb{R}^{J\times M}$ to denote the diffuse shading and the shadowing/masking terms under our J light sources yields

$$\mathbf{r} = \boldsymbol{\Psi}\boldsymbol{\gamma}. \qquad (5)$$

Assuming that the nanofacet distribution is isotropic, each element $\boldsymbol{\psi}$ is a 1D tabulated geometric attenuation factor $\boldsymbol{\psi} = \left[\frac{1}{\pi}, 0, \cdots, \frac{G(\mathbf{n},\mathbf{o},\mathbf{i})}{4(\mathbf{n}\cdot\mathbf{o})(\mathbf{n}\cdot\mathbf{i})}, \cdots, 0\right]^{\mathsf{T}} \in \mathbb{R}^M$. The first element in $\boldsymbol{\psi}$ is set to $\frac{1}{\pi}$, and the specular geometric factor $\frac{G(\mathbf{n},\mathbf{o},\mathbf{i})}{4(\mathbf{n}\cdot\mathbf{o})(\mathbf{n}\cdot\mathbf{i})}$ for the specular lobe is set to a position depending on the angle $\theta_{\mathbf{h}}$ between $\mathbf{n}$ and $\mathbf{h}$; the rest of elements is set to zero.

Furthermore, we factorize our reflectance into a linear combination of non-parametric basis BRDFs [Lawrence et al. 2006; Alldrin et al. 2008]. In particular, the *reflectance coefficient* vector $\boldsymbol{\gamma}$ can be represented as a linear combination of a number K of basis materials. We can rewrite $\boldsymbol{\gamma}$ as the product of the non-parametric basis BRDFs $\boldsymbol{\beta} \in \mathbb{R}^{M\times K}$ and their coefficients $\mathbf{w} \in \mathbb{R}^K$.

$$\boldsymbol{\gamma} = \boldsymbol{\beta}\mathbf{w}. \tag{6}$$

Substituting Equations (5) and (6) back to Equation (4), we have

$$\mathbf{l} = \boldsymbol{\phi} \odot (\boldsymbol{\Psi}\boldsymbol{\beta}\mathbf{w}), \tag{7}$$

which relates our unknown SVBRDF representation ($\boldsymbol{\beta}$ and $\mathbf{w}$) to the captured HDR images $\mathbf{l}$.

1.3 Microscale Reflectance and Normal Estimation

Alternating Solver We estimate microscale appearance from microscopic measurements in two steps. First, we initialize per-pixel normals. Then, we alternate the optimization of basis BRDFs $\boldsymbol{\beta}$, blending coefficients $\mathbf{w}$, and normals $\mathbf{n}$, based on the rendering equation for photometric consistency, minimizing the Euclidean error over the number of pixels N until convergence is reached:

$$\underset{\boldsymbol{\beta},\{\mathbf{w}_i\},\{\mathbf{n}_i\}}{\text{minimize}} \sum_{i=1}^{N} ||\mathbf{l}_i - \boldsymbol{\phi}_i \odot (\boldsymbol{\Psi}_i\boldsymbol{\beta}\mathbf{w}_i)||^2. \tag{8}$$

Initializing Normals The initial values of the normals are computed following the method of Tunwattanapong et al. [2013], exploiting the large number of point light sources in our setup. Specifically, the initial surface normal $\mathbf{n}$ at pixel $\mathbf{x}$ is computed from measurements under SH illumination (L3). The SH-based method allows us to measure the *first-surface* specular reflection that the microfacet theory stands on. However, since our lighting setup misses discrete SH illumination patterns around the zenith axis in about 20 degrees, the values $\mathbf{n}_\theta$ obtained in that area tend to be clamped in the SH-based approach. We thus take an algorithmic approach and employ shape-from-specularity (SfS) [Chen et al. 2006], interpolating mirror-like reflection vectors illuminated by point lights circling the edge of the area where information is missing. We then update the clamped zenith angles $\mathbf{n}_\theta$ and outlier artifacts estimated with interpolated normals from the SfS method.

Initializing $\mathbf{w}$ To initialize the spatial blending weight matrix $\mathbf{w}$, we cluster all pixels into K groups using the geometric mean of observations under varying light directions.

Updating $\boldsymbol{\beta}$ In order to solve the optimization problem of non-parametric bases $\boldsymbol{\beta}$, we pack measurements of $\boldsymbol{\Psi}$, $\mathbf{l}$ and $\boldsymbol{\Phi}$ for each pixel i in a form of $\mathbf{Hf} = \mathbf{g}$. Please see Figure 1 for a graphical illustration. $\mathbf{g} \in \mathbb{R}^{JN}$ is a column vector, whose elements represent radiance $\mathbf{l}_i$ under J lights for each pixel, and $\mathbf{f} \in \mathbb{R}^{MK}$ is another column vector obtained from vectorizing $\boldsymbol{\beta}$. We define $\mathbf{H} \in \mathbb{R}^{JN\times MK}$ as a matrix whose element $\mathbf{H}_i \in \mathbb{R}^{J\times MK}$ is a matrix of $\mathbf{w}_i{}^{\mathsf{T}} \otimes (\boldsymbol{\Phi}_i \odot \boldsymbol{\Psi}_i)$ for N number of pixels, where $\boldsymbol{\Phi}_i = [\boldsymbol{\phi}_i, \cdots, \boldsymbol{\phi}_i] \in \mathbb{R}^{J\times M}$ is the irradiance matrix that duplicates the elements $\boldsymbol{\phi}_i$ times the resolution M of the BRDFs, and $\otimes$ is the Kronecker product operator. The packing of $\mathbf{H}$ is inspired by a recent factorization method for non-parametric basis BRDFs [Alldrin et al. 2008]. Different from that work, we formulate $\mathbf{H}$ to factorize the nanofacet distribution function based on the Torrance-Sparrow model, rather than the entire basis BRDFs, in order to avoid overfitting in β. We then formulate an objective function $\mathcal{O}(\mathbf{f})$ that minimizes the squared difference between $\mathbf{Hf}$ and $\mathbf{g}$ solving $\mathcal{O}$ using quadratic programming. We use a sparse convex quadratic programming solver (e04nkc) provided by the Numerical Algorithms Group [NAG 2015]. In addition, linear constraints are set to impose non-negativity on $\boldsymbol{\beta}$, and the monotonicity of the distribution D. Note that we employ the monotonicity constraint only in the NDF optimization to preserve the pointy specular reflection phenomenon at the microscale following Ren et al. [2011]. We do not use a smoothness constraint, common in general optimization frameworks.

Updating $\mathbf{w}$ We can update $\mathbf{w}_i$ for each pixel i independently. The objective function is defined as

$$\mathcal{O}(\mathbf{w}) = \|\mathbf{l} - \{\boldsymbol{\phi} \odot (\boldsymbol{\Psi}\boldsymbol{\beta}\mathbf{w})\}\|^2. \tag{9}$$

In order to avoid overfitting $\mathbf{w}$ in our factorization, we consider a linear and a sparsity constraint: (a) the sum of non-negative blending weights $\mathbf{w}$ is forced to be equal or close to unity ($\sum \mathbf{w} \leqslant 1$), thus conserving energy; and (b) the weights $\mathbf{w}$ are forced to be a linear combination of relatively few basis BRDFs at each surface location. We solve the optimization by quadratic programming [NAG 2015].

Updating Normals For each pixel i, we compute a surface normal $\mathbf{n}_i$ that minimizes the l_2 norm of the difference between $\mathbf{l}$ and $\boldsymbol{\psi\gamma}$: $\|\mathbf{l} - \boldsymbol{\psi\gamma}\|$. In practice, we iteratively refine the interpolated normals using a multi-level grid approach [Chen et al. 2014]. At each iteration, we sample 3×3 normal candidates around the estimated normal, with one- or two-degree intervals over the hemisphere via concentric mapping. We then exhaustively search for an optimal normal that minimizes the error in Equation (8). Different from Chen et al. [2014], we reduce the angular search range by half at each stage, while preserving the same resolution of the grid. This multi-level grid approach allows us to find normals with a high angular resolution while searching the neighboring region within a certain boundary.

Termination Criteria Since we begin with a large amount of normal observations $\mathbf{n}$, we can safely assume that our initial normals are more accurate than the basis BRDFs $\boldsymbol{\beta}$ and coefficients $\mathbf{w}$. We first repeat our alternating optimization of $\boldsymbol{\beta}$ and $\mathbf{w}$ until they converge, then update $\mathbf{n}$ consequently and repeat the process. These

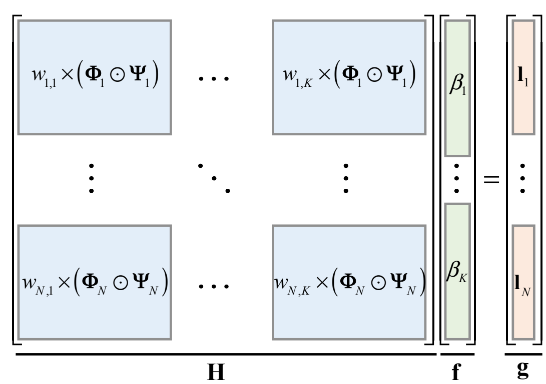

Figure 1: *Closed form matrix factorization to update* $\boldsymbol{\beta}$

alternating optimizations are conducted until the overall radiance error converges in Equation (8).

Color in SVBRDF According to the microfacet theory, the specular distribution is determined by the first-surface roughness, which is monochromatic. Only Fresnel effects in the specular reflection influence color in case of metallic surfaces. Accordingly, our formulation the distribution of nanofacets D and specular scaling coefficient ρ_s are monochromatic in Equation (1), while diffuse albedo ρ_d and Fresnel F are chromatic. Our non-parametric basis $\boldsymbol{\beta}$ includes the mixture of monochromatic and chromatic properties. To represent color, we first factorize three color channels individually to obtain red, green and blue $\boldsymbol{\beta}$ [Lawrence et al. 2006; Weistroffer et al. 2007; Alldrin et al. 2008]. Different from previous works, we then extract monochromatic D and ρ_s from each $\boldsymbol{\beta}$ via D normalization to utilize them for rendering (see Section 1.2). Most materials present common D and ρ_s across color channels. In practice, we found that estimates using the green channel are more reliable than others. Once each estimation of D and ρ_s is done, we share the green channel's estimate as representative, while we preserve the original colorimetric properties ρ_d and F from each channel's basis BRDF $\boldsymbol{\beta}$ to present color appearance.

References

AITTALA, M., WEYRICH, T., AND LEHTINEN, J. 2013. Practical SVBRDF capture in the frequency domain. *ACM Trans. Graph. 32*, 4, 110:1–12.

ALLDRIN, N., ZICKLER, T., AND KRIEGMAN, D. 2008. Photometric stereo with non-parametric and spatially-varying reflectance. In *Proc. IEEE CVPR 2008*, 1–8.

ASHIKHMIN, M., PREMOZE, S., AND SHIRLEY, P. 2000. A microfacet-based BRDF generator. In *Proc. ACM SIGGRAPH 2000*, 65–74.

CHEN, T., GOESELE, M., AND SEIDEL, H.-P. 2006. Mesostructure from specularity. In *Proc. IEEE CVPR 2006*, 1825–1832.

CHEN, G., DONG, Y., PEERS, P., ZHANG, J., AND TONG, X. 2014. Reflectance scanning: estimating shading frame and BRDF with generalized linear light sources. *ACM Trans. Graph. 33*, 4, 117:1–11.

COOK, R. L., AND TORRANCE, K. E. 1982. A reflectance model for computer graphics. *ACM Trans. Graph. 1*, 1, 7–24.

HOLROYD, M., LAWRENCE, J., HUMPHREYS, G., AND ZICKLER, T. 2008. A photometric approach for estimating normals and tangents. *ACM Trans. Graph. 27*, 5, 133.

LAWRENCE, J., BEN-ARTZI, A., DECORO, C., MATUSIK, W., PFISTER, H., RAMAMOORTHI, R., AND RUSINKIEWICZ, S. 2006. Inverse shade trees for non-parametric material representation and editing. *ACM Trans. Graph. 25*, 3, 735–745.

NAG, 2015. The NAG Library, Numerical Algorithms Group. `http://www.nag.com/`.

NGAN, A., DURAND, F., AND MATUSIK, W. 2005. Experimental Analysis of BRDF Models. *Rendering Techniques 2005*, 16.

REN, P., WANG, J., SNYDER, J., TONG, X., AND GUO, B. 2011. Pocket reflectometry. *ACM Trans. Graph. 30*, 4, 45:1–10.

TORRANCE, K. E., AND SPARROW, E. M. 1967. Theory for off-specular reflection from roughened surfaces. *JOSA 57*, 9, 1105–1112.

TUNWATTANAPONG, B., FYFFE, G., GRAHAM, P., BUSCH, J., YU, X., GHOSH, A., AND DEBEVEC, P. 2013. Acquiring reflectance and shape from continuous spherical harmonic illumination. *ACM Trans. Graph. 32*, 4, 109:1–12.

WANG, C.-P., SNAVELY, N., AND MARSCHNER, S. 2011. Estimating dual-scale properties of glossy surfaces from step-edge lighting. *ACM Trans. Graph. 30*, 6, 172.

WEISTROFFER, R. P., WALCOTT, K. R., HUMPHREYS, G., AND LAWRENCE, J. 2007. Efficient basis decomposition for scattered reflectance data. In *Proc. Eurographics*, 207–218.